
ENTROPY TRAJECTORY SHAPE PREDICTS LLM REASONING RELIABILITY: A DIAGNOSTIC STUDY OF UNCERTAINTY DYNAMICS IN CHAIN-OF-THOUGHT

A PREPRINT

Xinghao Zhao

Huazhong University of Science and Technology
xinghaozhao60@gmail.com

March 20, 2026

ABSTRACT

Chain-of-thought (CoT) reasoning improves LLM accuracy on complex tasks, yet reliable methods for detecting reasoning failures without expensive multi-sample approaches remain elusive. We study whether the *shape* of uncertainty dynamics across reasoning steps—captured cheaply by sampling a handful of answer completions at each step—predicts whether the final answer is correct.

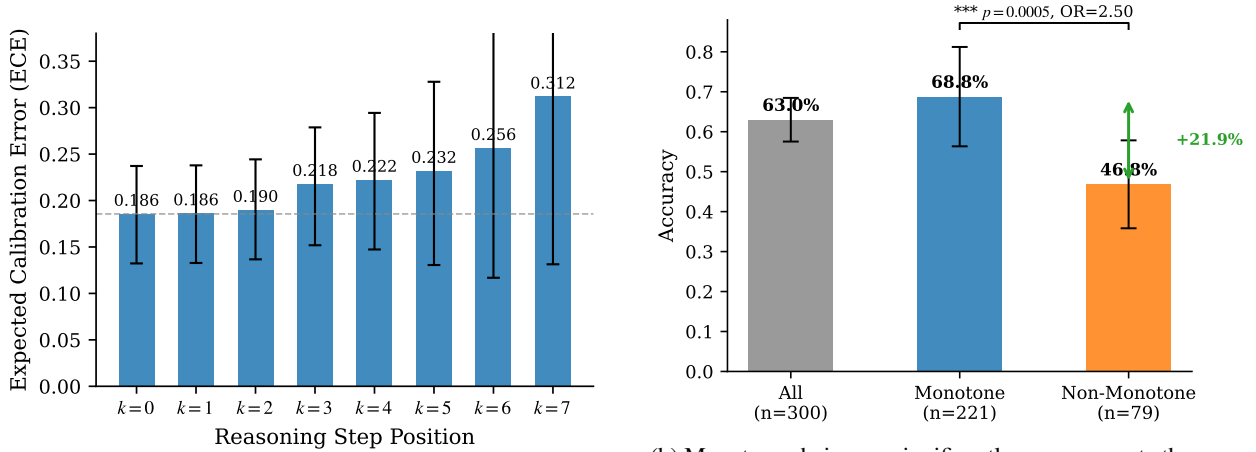
We introduce the concept of *entropy-trajectory monotonicity*: a chain is monotone if its per-step answer-distribution entropy decreases at every step, reflecting consistent uncertainty reduction. On GSM8K ($n=300$) with Qwen2.5-7B-Instruct, monotone chains achieve 68.8% accuracy versus 46.8% for non-monotone chains—a gap of +21.9 percentage points (Fisher’s exact $p=0.0005$; OR= 2.50). Critically, the *scalar* total entropy reduction is not predictive ($\rho=-0.06$, $p=0.31$), revealing a *shape-over-magnitude dissociation*: it is *whether* entropy decreases at every step, not *how much* it drops, that predicts correctness. The dissociation extends to the graded signal: violation count 0/1/2 corresponds to 68.8%/50.8%/28.6% accuracy, while violation magnitude is uninformative.

We further show that token log-probability confidence worsens in calibration with step depth (ECE: 0.186 \rightarrow 0.312 from step 0 to step 7), and that entropy-trajectory monotonicity achieves +5.8 pp at 73.7% coverage, outperforming all scalar baselines including final-step entropy (+2.2 pp) and scalar coherence (−0.6 pp, worse than random) at $\approx 1,500$ tokens/question— one-eighth the cost of 40-chain self-consistency. These findings, obtained on a single model and dataset as a diagnostic pilot, replicate on a second model (Mistral-7B-Instruct-v0.3, $n=300$), where monotone chains reach 72.3% vs. 37.6% for non-monotone chains (+34.7 pp; OR= 4.33). Structural properties of uncertainty trajectories are thus more informative than aggregate magnitude measures across model families.

1 Introduction

Large language models (LLMs) produce correct and incorrect answers with equal surface fluency. In chain-of-thought (CoT) reasoning [Wei et al., 2022, Kojima et al., 2022], a model generates a multi-step solution before giving a final answer—but a confident-looking chain of steps offers no guarantee of correctness. Detecting failures cheaply, without generating many independent samples, is an open practical problem.

Two families of reliability signals have been studied. *Self-consistency* methods [Wang et al., 2023] aggregate answers from multiple independently sampled chains, but require 10–40 samples per question and discard the rich step-level information within each chain. *Token log-probability* scores are cheap but systematically miscalibrated: we show that the ECE of token log-prob confidence increases from 0.186 at the first reasoning step to 0.312 at the eighth step (Figure 1a), with all standard proxy functions collapsing to near-degenerate confidence ranges.



(a) ECE increases monotonically with step depth (0.186 at step 0 to 0.312 at step 7). Error bars show 95% bootstrap CIs.

(b) Monotone chains are significantly more accurate than non-monotone chains (OR= 2.50, Fisher’s $p=0.0005$, +21.9 pp gap).

Figure 1: Two key findings from our diagnostic study. **(a)** Token log-probability confidence becomes increasingly miscalibrated at later reasoning steps. **(b)** Chains with monotone entropy trajectories achieve substantially higher accuracy than non-monotone chains.

We pursue a different approach: rather than scoring a chain by a single scalar derived from token probabilities, we ask how the model’s uncertainty over the *final answer* evolves step by step. At each step prefix, we sample $m=5$ answer completions and compute the Shannon entropy H_k of the resulting answer distribution. This gives an *entropy trajectory* (H_0, H_1, \dots, H_N) at low additional cost.

The central question we study is: does the *shape* of this trajectory predict correctness, beyond what its *magnitude* can explain?

Main finding. On GSM8K ($n=300$; Qwen2.5-7B-Instruct), chains whose entropy trajectory is monotonically decreasing achieve 68.8% accuracy, versus 46.8% for non-monotone chains—a gap of +21.9 pp (95% CI: [+9.5, +34.3]; Fisher’s exact $p=0.0005$; OR= 2.50; Figure 1b). In contrast, the total entropy drop $H_0 - H_N$ (scalar coherence) has near-zero correlation with correctness (Spearman $\rho=-0.06$, $p=0.31$). Whether uncertainty decreases *consistently*—not how much it drops overall—is the operative signal.

Contributions. This paper is a *diagnostic study*: we introduce a new signal, establish its empirical properties on GSM8K with Qwen2.5-7B, and characterize its failure modes. We further replicate the effect on a second model family (Mistral-7B-Instruct-v0.3) and provide an initial benchmark extension to MATH (Sections A.16 and A.17). Concretely, we contribute:

1. **Shape-over-magnitude dissociation.** Binary entropy-trajectory monotonicity is a strong predictor (OR= 2.5, $p=0.0005$), while the scalar total entropy drop is not ($\rho=-0.06$). The dissociation extends to a graded signal: violation count 0/1/2 \rightarrow 68.8%/50.8%/28.6% accuracy, while violation magnitude is uninformative.
2. **Step-level calibration worsens with depth.** Token log-prob ECE rises from 0.186 at step 0 to 0.312 at step 7—the reverse of what one might expect as the model approaches its final answer.
3. **Selective prediction vs. cheap baselines.** Entropy-trajectory monotonicity achieves +5.8 pp at 73.7% coverage, outperforming all scalar baselines (final-step entropy +2.2 pp; scalar coherence -0.6 pp, worse than random; chain length +2.6 pp), at $\approx 1,500$ tokens/question.
4. **Extensive ablations and robustness checks.** Results are stable across $m \in \{3, 5, 10\}$ samples/step (gap variation < 1.5 pp), $\varepsilon \in [0, 0.10]$ (+21.9 pp unchanged), sampling temperature $\tau \in \{0.3, 0.5, 0.7, 1.0\}$ (gap range +14.4–+23.1 pp, all substantially positive), and are confirmed after Miller–Madow bias correction and confounder control (Sections A.1, A.2, A.7, A.9 and A.15). The result is also robust to step-segmentation: restricting to the 96.7% of chains with $N \geq 3$ steps yields an identical +21.9 pp gap (Section A.13). The step-depth ECE trend is confirmed under equal-mass binning (Section A.14).

The remainder of this paper is organized as follows. Section 2 describes our experimental setup and defines the key metrics. Section 3 presents step-level calibration results. Section 4 presents the entropy trajectory analysis. Section 5 situates our work in the literature. Section 6 concludes.

2 Setup and Methods

Model and dataset. We use Qwen2.5-7B-Instruct [Team, 2024] with the model’s native chat template applied via `tokenizer.apply_chat_template`—a detail that matters: using raw text prompting instead reduces GSM8K accuracy from $\sim 63\%$ to $\sim 38\%$ on this model. We evaluate on a random sample of $n=300$ problems from the GSM8K test split [Cobbe et al., 2021], a standard benchmark of grade-school arithmetic word problems requiring multi-step reasoning.

Chain-of-thought generation. For each problem, we generate one CoT chain (temperature $\tau=0.1$, max 512 tokens). The chain is segmented into steps by matching patterns of the form “Step k :” in the generated text, with a sentence/newline fallback for problems that do not produce explicit step markers. Token log-probabilities are recorded at generation time for calibration analysis.

Step-level entropy measurement. At each step prefix $s_0s_1 \cdots s_k$, we sample $m=5$ answer completions (temperature $\tau=0.7$, max 150 tokens) and extract final numerical answers. The temperature $\tau=0.7$ introduces diversity in completions so that entropy $H_k > 0$ when the model is uncertain; lower temperatures would underestimate uncertainty, and higher temperatures add noise unrelated to the model’s actual uncertainty. Ablations over $m \in \{3, 5, 10\}$ and $\tau \in \{0.3, 0.5, 0.7, 1.0\}$ are reported in Sections A.1 and A.2. The per-step answer entropy is:

$$H_k = - \sum_{a \in \mathcal{A}} \hat{p}_k(a) \log \hat{p}_k(a), \quad (1)$$

where $\hat{p}_k(a)$ is the empirical frequency of answer a in the m samples at step k . This gives an entropy trajectory (H_0, H_1, \dots, H_N) for each chain of N steps.

Scalar coherence. The scalar coherence score is $\mathcal{C} = H_0 - H_N$: the total entropy drop from the start to the end of the chain. A high value indicates that, overall, the model became more certain about the answer across the reasoning chain.

Binary monotonicity. A chain is ε -monotone if its entropy trajectory decreases at every step up to a small tolerance:

$$H_{k+1} \leq H_k + \varepsilon \quad \text{for all } k \in \{0, \dots, N-1\}, \quad (2)$$

where $\varepsilon \geq 0$ controls sensitivity to negligible fluctuations. We use $\varepsilon=0.01$ as the primary threshold; this is a per-step additive tolerance on entropy (measured in nats), not a cumulative bound. A chain is *non-monotone* if any single step violates Equation (2). Strict monotonicity ($\varepsilon=0$) is the limiting case.

Step-level calibration. Token log-probabilities are aggregated per step as the mean log-probability $\bar{\ell}_k$ of tokens in step k . We compare four confidence proxy functions mapping $\bar{\ell}_k$ to $[0, 1]$: sigmoid-shifted ($\sigma(\bar{\ell} + 1.5)$), sigmoid-unshifted ($\sigma(\bar{\ell})$), raw-logprob (linear normalization), and $\exp(\bar{\ell})$. For each proxy, we compute the Expected Calibration Error (ECE) [Naeini et al., 2015, Guo et al., 2017] at each step position k using 10 equal-width bins, with 95% bootstrap confidence intervals over $B=500$ resamples.

Selective prediction. We evaluate the practical utility of the monotonicity signal by using it as a coverage filter: the model “answers” only the subset of problems whose chain is monotone and abstains on the rest. We report accuracy at this coverage level and plot accuracy as a function of coverage under two ranking strategies: (1) sorting by binary monotonicity first, then by scalar coherence; (2) sorting by scalar coherence alone.

3 Step-Level Calibration

ECE increases monotonically with step depth. Table 1 summarizes four token log-probability confidence proxies and the answer-distribution confidence proxy at step position $k=0$. Figure 1a shows the ECE of the sigmoid-shifted proxy at each step position $k=0, \dots, 7$ (positions with fewer than 10 observations are excluded). ECE rises from 0.186 at step 0 to 0.312 at step 7—a 68% relative increase. The trend is monotone across all eight positions, though a formal Spearman test on $n=8$ step bins is underpowered ($\rho=0.27$, $p=0.45$). Equal-mass (decile) binning confirms the trend, with ECE values $0.195 \rightarrow 0.357$ (step 0 \rightarrow 7); see Section A.14 for a step-by-step comparison.

Table 1: Confidence proxies for step-0 correctness prediction ($n=300$). ECE: Expected Calibration Error; AUROC: area under ROC; ρ : Spearman correlation with final answer correctness. All token log-probability proxies produce identical Spearman rankings and collapsed confidence ranges.

Confidence Proxy	ECE ↓	AUROC ↑	ρ	Conf. Range
$\sigma(\bar{\ell} + 1.5)$ (sigmoid-shifted)	0.186	—	+0.166**	[0.802, 0.818]
$\sigma(\bar{\ell})$ (sigmoid-unshifted)	0.133	—	+0.166**	[0.475, 0.500]
$\bar{\ell}$ (raw-logprob, normalized)	0.265	—	+0.166**	[0.990, 1.000]
$\text{exp}(\bar{\ell})$ (exp-logprob)	0.254	—	+0.166**	[0.906, 1.000]
Majority-vote rate (answer-dist)	0.251	0.547	+0.084	[0.144, 0.749]

** $p < 0.01$; all four token log-prob

proxies have identical Spearman ρ (same logprob ordering).

Token log-prob proxies share ranking but compress confidence range. All four token log-probability proxies produce identical Spearman correlations with correctness ($\rho = +0.166$, $p = 0.004$), because they are all strictly monotone transformations of the same underlying log-probability values—they yield the same ranking over problems. More importantly, their confidence *ranges* collapse due to the normalization choices: the sigmoid-shifted proxy assigns all 300 problems confidences in [0.802, 0.818], a range of only 0.016, while the raw-logprob proxy collapses to [0.990, 1.000]. This range compression is a property of the chosen transformations combined with the token-probability regime, not an intrinsic flaw of log-probs as a signal. The practical consequence is that ECE metrics reflect the mean confidence vs. empirical accuracy gap rather than discrimination failure: models assign token-level log-probabilities in a narrow regime that maps to above 0.8 after standard transformations, regardless of whether the answer is correct.

Answer-distribution confidence. The majority-vote rate computed from the $m=5$ per-step samples (answer-dist proxy) avoids this structural collapse, with confidence values spanning [0.14, 0.75]. However, its predictive power is weak: ECE = 0.251, AUROC = 0.547, Spearman $\rho = +0.084$ ($p = 0.15$, not significant). The answer-distribution *scalar* at step 0 provides limited calibration.

Interpretation. The step-level ECE trend suggests that token log-probability confidence—already poorly calibrated at step 0—becomes progressively worse as reasoning progresses. This is counterintuitive: one might expect a model to become *better* calibrated as it approaches the final answer. The ECE increase is driven by models becoming effectively more overconfident at later steps (the mean confidence remains nearly constant while empirical accuracy varies), not by any increase in probability variance. We interpret this as a descriptive observation requiring further investigation across models and datasets.

A natural question is whether the answer-distribution at step k is better calibrated to *step- k intermediate correctness* than to final-answer correctness. This would require step-level correctness labels, which are unavailable in our unsupervised setup; assigning them requires a process reward model [Lightman et al., 2023] or human annotation. We therefore use final-answer correctness as the only available calibration target, which we acknowledge is a mismatch for early steps. Under this framing, our ECE curves should be interpreted as *predictive calibration* of eventual success, not as direct evidence about step-local correctness calibration. The fact that the answer-distribution scalar MVR_k at step 0 achieves only AUROC = 0.547 for final correctness confirms that single-step scalars provide limited calibration signal—motivating the trajectory-shape analysis of Section 4.

4 Entropy Trajectory Dynamics

Scalar coherence is not predictive. The scalar coherence $\mathcal{C} = H_0 - H_N$ (total entropy drop) has Spearman $\rho = -0.059$ with final answer correctness ($p = 0.31$; not significant). Correct answers are associated with *lower* total entropy reduction than incorrect ones (mean coherence: 0.59 correct vs. 0.68 incorrect; gap = -0.088). This counterintuitive direction reflects cases where incorrect chains converge quickly to a wrong answer—showing a large apparent coherence—while correct chains may deliberate longer with more moderate convergence.

Binary monotonicity is a strong predictor. Among the 300 evaluated chains, 221 (73.7%) are monotone by the criterion in Equation (2). Table 2 and Figure 1b show the main result:

The accuracy gap of +21.9 pp is statistically robust (95% CI: [+9.5, +34.3] via stratified bootstrap; Fisher’s exact $p = 0.0005$; OR = 2.50).

Table 2: Accuracy by entropy-trajectory monotonicity on GSM8K ($n=300$, Qwen2.5-7B-Instruct). CI is 95% bootstrap; p is Fisher’s exact test.

Subset	n	Accuracy	95% CI	Fisher’s p / OR
All chains	300	63.0%	—	—
Monotone chains	221	68.8%	[63.0, 74.7]	$p=0.0005$ / OR= 2.50
Non-monotone chains	79	46.8%	[35.7, 57.9]	—
Accuracy gap (monotone – non-monotone)			+21.9 pp	[+9.5, +34.3]

As an additional robustness check, a 3-seed sweep under the same run-configuration yields consistently positive monotone/non-monotone gaps (mean +9.1 pp; range +5.2 to +13.8 pp; details in Section A.18). Using a difficulty proxy control that includes SC@3 agreement, chain length, and question length, monotonicity remains an independent positive predictor (OR \approx 2.37; Section A.8).

Cross-model replication on Mistral-7B. We replicate the GSM8K experiment with Mistral-7B-Instruct-v0.3 ($n=300$, same sampling setup and seed). The shape signal remains strong and significant: monotone chains achieve 72.3% accuracy vs. 37.6% for non-monotone chains, for a +34.7 pp gap (OR= 4.33, Fisher’s $p<10^{-8}$), at monotone coverage 39.7% (details in Section A.17). While absolute accuracies differ across model families, the core shape-over-magnitude effect persists.

Shape-over-magnitude dissociation. The contrast between the null scalar result ($\rho=-0.06$) and the significant binary result (OR= 2.50, $p=0.0005$) reveals a *shape-over-magnitude dissociation*: whether entropy decreases at every step (shape) predicts correctness; how much it drops in total (magnitude) does not.

The dissociation is conceptually informative. A chain that drops entropy sharply, then rises on encountering a difficult sub-step, then drops again may exhibit a large total coherence \mathcal{C} while its non-monotone dynamics signal mid-chain confusion. Conversely, a chain with a small but steady entropy decrease at every step is monotone, indicating the model never “changes its mind” about the answer direction.

Failure mode analysis. Monotonicity is a diagnostic, not a perfect oracle. Of the 221 monotone chains, 69 (31.2%) are *false positives*: monotone but incorrect. Of the 79 non-monotone chains, 42 (53.2%) are *false negatives*: non-monotone but correct. As a classifier for final correctness, monotonicity has precision 68.8% (152/221), recall 80.4% (152/189), and F1 74.1%. The signal is thus most useful as a triage filter—flagging likely-wrong answers for re-sampling or abstention—rather than as a high-precision correctness certificate. One natural extension is to combine monotonicity with complementary signals (e.g., final-answer confidence from token log-probabilities or majority-vote rate) in a lightweight scoring rule; such combinations could reduce the false-positive rate at comparable coverage.

Qualitative examples. Figure 2 shows representative entropy trajectories. The monotone chain shows a smooth decrease: each additional step reduces uncertainty. The non-monotone chain shows an entropy spike at step 2—a point where the model introduces an intermediate calculation that conflicts with its later reasoning—before partially recovering.

Selective prediction and baseline comparison. Table 3 compares entropy-trajectory monotonicity against seven cheap baselines at 73.7% coverage. Monotonicity achieves +5.8 pp over full coverage (AURC = 0.311), outperforming final-step entropy (+2.2 pp, AURC = 0.313) and chain-length triage (+2.6 pp, AURC = 0.310). The reviewer-requested single-trajectory baselines are weak in this setup: self-judgment with one short verifier call reaches 62.4% (AURC = 0.368, $\rho=+0.019$), and strict Yes/No self-evaluation reaches 63.3% (AURC = 0.395, $\rho=-0.019$), both well below trajectory-shape signals (protocol in Section A.21). Scalar coherence is also *worse than random* (−0.6 pp), confirming the shape-over-magnitude dissociation. Figure 3 shows the full accuracy-coverage curves.

Violation count as a graded signal. The binary monotonicity flag (violation count = 0) is a zero-threshold discretization of the continuous violation count $v = \sum_k \mathbf{1}[H_{k+1} > H_k + \varepsilon]$. The graded signal reveals additional structure beyond the binary split: chains with zero violations achieve 68.8% accuracy, those with exactly one violation achieve 50.8%, and those with two or more violations achieve 28.6% — a monotonically decreasing progression (Section A.12). Violation count achieves Spearman $\rho=+0.209$ ($p=0.0003$), marginally stronger than binary monotonicity ($\rho=+0.200$), while achieving identical AURC = 0.311. Crucially, the *magnitude* of violations does not add predictive value: among non-monotone chains, the max positive ΔH has Spearman $\rho=-0.017$ ($p=0.88$) with correctness, confirming that

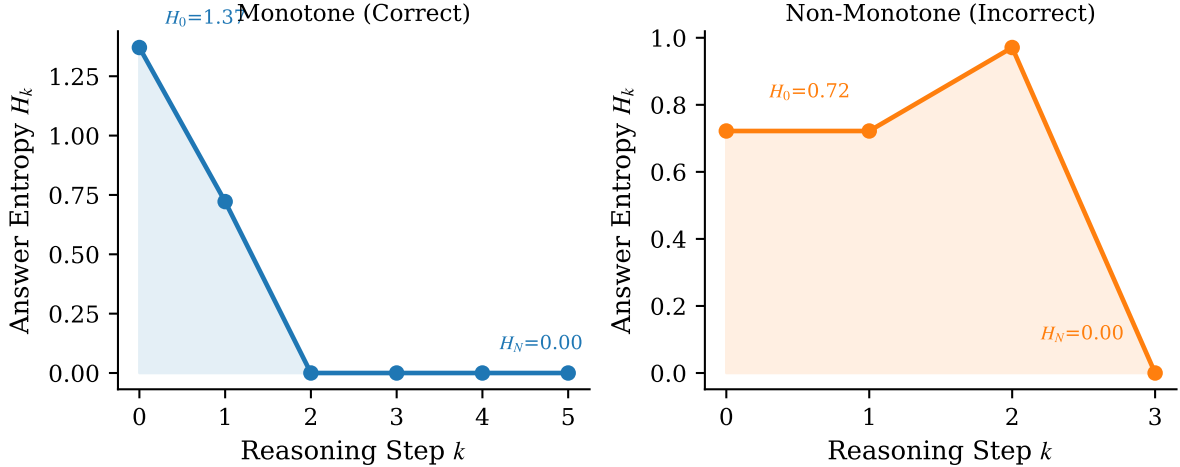


Figure 2: Example per-step answer-distribution entropy trajectories. **Left:** A monotone trajectory (each step reduces H_k), corresponding to a correct final answer. **Right:** A non-monotone trajectory with a mid-chain entropy spike, corresponding to an incorrect answer. H_k is defined in Equation (1).

Table 3: Cheap reliability signals on GSM8K ($n=300$). Coverage fixed at 73.7% ($k=221$). AURC: area under risk-coverage curve (lower is better; random ≈ 0.398 , oracle = 0.068). *: $p<0.05$; **: $p<0.01$.

Signal	Acc@73.7%	Δ	Spearman ρ	AURC
Random	62.9%	-0.1 pp	0.000	0.398
Chain length (shorter first)	65.6%	+2.6 pp	+0.101	0.310
Final-step entropy H_N	65.2%	+2.2 pp	+0.093	0.313
Scalar coherence $H_0 - H_N$	62.4%	-0.6 pp	-0.059	0.408
Self-judgment (1 verifier call)	62.4%	-0.6 pp	+0.019	0.368
Yes/No self-eval ($P(\text{Yes})$)	63.3%	+0.3 pp	-0.019	0.395
Max positive ΔH	68.8%	+5.8 pp	+0.135*	0.340
Violation count (-vc)	68.8%	+5.8 pp	+0.209**	0.311
Entropy monotonicity (ours)	68.8%	+5.8 pp	+0.200**	0.311

how many disruptions occur matters, not how large they are. This is a direct extension of the shape-over-magnitude dissociation to the multi-violation setting.

Token budget and equal-budget self-consistency. Our method uses $m \times \bar{N} \approx 5 \times 4.9 \approx 25$ short completions (max 150 tokens) per question, totaling $\approx 1,500$ tokens—*two times cheaper* than 10-chain self-consistency ($\approx 3,000$ tokens) and *eight times cheaper* than 40-chain self-consistency ($\approx 12,000$ tokens). We now run empirical equal-budget baselines on the same 300 GSM8K problems (Table 14). Under near-equal cost to our method, SC@5 uses 1385.7 tokens/problem on average and reaches 65.3% accuracy. SC@3 uses 831.4 tokens/problem with 66.0% accuracy. An ESC-style early-stop simulation reaches 66.3% accuracy at only 673.6 tokens/problem, stopping after 2.35 chains on average. For reference, our monotonicity-gated policy yields 68.8% accuracy on the answered subset (73.7% coverage) with $\approx 1,500$ tokens/problem. These empirical results replace the previous argument-only comparison and show that full-chain voting improves over greedy decoding, while ESC offers a stronger efficiency-accuracy trade-off among SC-style baselines. To provide a matched-target comparison, we additionally compute coverage-aware SC curves by ranking SC outputs with vote-agreement confidence. At 73.7% coverage, SC@3 and SC@5 reach 70.6% and 69.7% answered-set accuracy, respectively, compared with 68.8% for our monotonicity ranking (details in Section A.20, including a unified matched-coverage comparison figure). To avoid metric mismatch, we report both coverage-aware and full-coverage views: our 68.8% number is answered-set accuracy at 73.7% coverage, whereas SC/ESC numbers are full-coverage accuracies. Token accounting is likewise split into (i) measured full-chain costs for SC/ESC and (ii) component-wise accounting for our method (base-chain measured, per-step sampling term explicitly parameterized); see Section A.22 for the full breakdown and assumptions.

Equal-budget fairness clarification. We compare two evaluation targets on purpose: selective performance for our method (answered-set accuracy at fixed coverage) versus full-coverage performance for SC/ESC (all-problem accuracy).

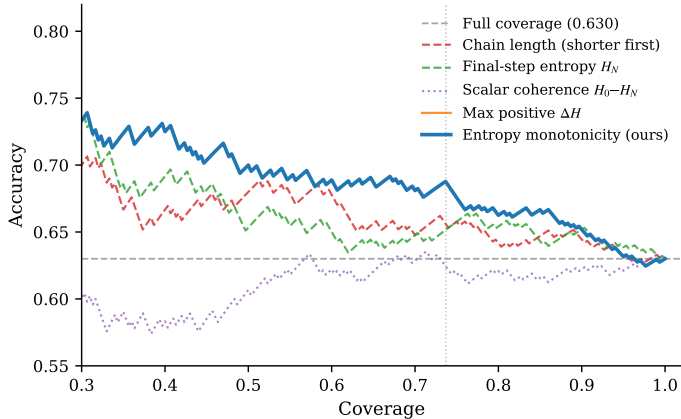


Figure 3: Accuracy vs. coverage for five cheap reliability signals. Entropy-trajectory monotonicity (solid blue) dominates all scalar baselines. Scalar coherence (dotted, AURC = 0.408) is below the random baseline. Dashed line: full-coverage accuracy (63.0%).

The budgets are also tied to different operational goals: our method spends tokens on per-step short completions to rank and abstain, while SC/ESC spend tokens on additional full-chain samples to vote before answering every problem. To provide a fair empirical anchor rather than only theoretical scaling arguments, we report executed SC@3, SC@5, and ESC-sim runs on the same 300-problem split with measured token costs (Table 14 and Section A.22).

Early-step monotonicity for compute-aware triage. Prefix-only variants already provide useful separation. Using only the first $k=2$ entropy transitions, prefix monotonicity achieves a +16.7 pp accuracy gap (65.7% vs. 49.0%) on the $n=290$ problems with at least two transitions, while using only $0.60\times$ the full trajectory cost on average (Section A.4). On the same subset, full-trajectory monotonicity gives +21.9 pp, so the $k=2$ rule recovers about 76% of the full gap at substantially lower cost. This supports an early-exit deployment mode where problems are triaged after the first two transitions and only ambiguous cases are expanded to full trajectories.

5 Related Work

Step-level signals for CoT reasoning. Recent work has begun exploring step-resolution information in CoT generation. ConfSpec [Liu and He, 2026] uses per-step token confidence to trigger early exit for speculative reasoning, accelerating inference without explicit reliability modeling. Concurrent work uses step-level confidence signals for RL fine-tuning of reasoning chains [Cai and Sugiyama, 2026]. Our work differs in goal: we study uncertainty dynamics within a single chain for *diagnostic* purposes, without any training. Our work also differs in granularity from studies that aggregate across multiple sampled CoT paths: we analyze trajectory shape *within* a single chain rather than across parallel chains.

Active-Prompt [Diao et al., 2023] selects few-shot exemplars based on final-answer disagreement/entropy over multiple sampled chains, showing that answer-distribution entropy at the *output* is informative for difficulty estimation. Our work complements this by studying entropy dynamics *within* a single chain rather than across chains, and by showing that the shape of the trajectory (not just the terminal value) carries diagnostic value. Self-evaluation guided decoding [Xie et al., 2023] integrates step-wise correctness signals into beam search; process reward models [Lightman et al., 2023, Uesato et al., 2022] supervise reasoning at step resolution using labeled data. In contrast, our method is fully unsupervised and requires only inference, making it applicable without any labeled process data.

Self-consistency and sampling-based reliability. The dominant approach to reliability estimation is self-consistency [Wang et al., 2023]: generating multiple independent CoT chains and taking the majority answer. Extensions include complexity-based weighting [Fu et al., 2023] and universal self-consistency [Chen et al., 2023]. These methods require 10–40 samples per question and discard the step-level structure within each chain. Early-stopping self-consistency (ESC; Li et al. 2024) reduces this cost by stopping sampling once a majority is detected, but still operates at the level of full chains and provides no step-level diagnostic. Our approach generates $m=5$ short completions per step (not full chains), providing step-resolution information at $\approx 1,500$ tokens per problem—one-fifth the cost of SC-10 and one-eighth of SC-40. The key distinction is that we use the *trajectory shape* of within-chain sampling as a reliability signal, rather than across-chain majority vote.

Xiong et al. [2026] addresses the complementary question of *when* to invoke multi-path reasoning based on single-trajectory features, using learned sampling controllers. Our method provides a cheap, unsupervised alternative based purely on entropy dynamics, without requiring any training.

Single-trajectory reliability signals. Several recent works propose lightweight single-chain reliability signals. Xie et al. [2026] introduce anchor-token confidence: a model’s probability on a single Yes/No self-evaluation token as a reliability indicator. This signal is extremely cheap (one forward pass) but discards the temporal structure of the reasoning chain. Our entropy-trajectory monotonicity captures richer information by tracking uncertainty *evolution* across steps, at the cost of $m=5$ short completions per step. Ghasemabadi and Niu [2025] study whether LLMs can predict their own failures via self-judging, finding moderate success that complements structural signals. White-box correctness verification (CRV; Zhao et al. 2026) exploits the computation graph of the reasoning chain for verification, achieving higher accuracy than sampling-based approaches but requiring access to model internals and substantial compute. Our method is fully black-box, requiring only the ability to generate completions from a prefix.

Temporal confidence dynamics. Several recent works explicitly model confidence as a temporal process. Temporalizing Confidence [Mao et al., 2025] formulates stepwise confidence trajectories with Signal Temporal Logic constraints (including monotonicity-like templates), but operates on token-level confidence traces and requires richer control over confidence shaping. Recurrent Confidence Chain [Mao and Venkat, 2026] aggregates step confidence with a temporal recurrent mechanism informed by inter-step dependencies, improving calibration at the cost of additional modeling assumptions. Thought Calibration [Wu et al., 2025] focuses on confidence-driven test-time stopping with lightweight probes on hidden representations. Compared with these methods, our approach is deliberately minimal: fully unsupervised, black-box, and based only on sampled answer distributions from prefix completions.

Process reward models. Supervised process reward models (PRMs) assign credit to intermediate steps using human annotations [Lightman et al., 2023] or automated annotations [Uesato et al., 2022, Wang et al., 2024]. PRMs require training and labeled process data; our entropy-trajectory approach is fully unsupervised and requires only inference. The monotonicity signal can be viewed as a cheap proxy for process supervision: a chain that never increases uncertainty about its answer is unlikely to contain a mid-chain error.

LLM calibration. A substantial body of work studies the calibration of LLM predictions at the output level [Guo et al., 2017, Kadavath et al., 2022, Xiong et al., 2024]. Kadavath et al. [2022] show that LLMs can express calibrated uncertainty about factual knowledge through self-evaluation. Xiong et al. [2024] survey calibration methods for LLMs, including temperature scaling and verbal confidence elicitation. Our work differs in studying how calibration evolves *within* a reasoning chain—a temporal dimension absent from final-answer calibration studies—and in observing that token log-probability confidence worsens with step depth.

6 Conclusion

We studied whether the shape of answer-distribution entropy dynamics across reasoning steps predicts the correctness of chain-of-thought outputs. On GSM8K with Qwen2.5-7B-Instruct, we found a clear shape-over-magnitude dissociation: binary entropy-trajectory monotonicity is a significant predictor of correctness (OR= 2.50, Fisher’s $p=0.0005$, +21.9 pp accuracy gap), while the scalar total entropy drop is not ($\rho=-0.06$, $p=0.31$). Token log-probability confidence worsens in calibration from the first to the last reasoning step, and monotonicity-based selective prediction achieves +5.8 pp accuracy at 73.7% coverage. The same directional effect replicates on Mistral-7B-Instruct-v0.3 with an even larger gap (+34.7 pp; OR= 4.33), supporting cross-family robustness.

Limitations. This study remains limited in breadth despite the second-model replication. An initial generalization experiment on MATH [Hendrycks et al., 2021] (Level 1–3 subset, $n=200$) shows the same directional effect—monotone chains achieve +8.1 pp higher accuracy than non-monotone chains—though the gap is smaller than on GSM8K, consistent with MATH being harder and answer formats more varied (Section A.16). On GSM8K, replication on Mistral-7B-Instruct-v0.3 confirms the core signal (Section A.17), but broader model coverage (e.g., Phi-3, Gemma, Llama variants) is still needed. Temperature ablations ($\tau \in \{0.3, 0.5, 0.7, 1.0\}$) confirm that the +21.9 pp gap is robust across sampling temperatures (Section A.1). Threshold robustness and confounder control analyses (Sections A.7 and A.9) show that the +21.9 pp gap is unchanged for all $\varepsilon \leq 0.10$ and that partial correlation controlling for chain length remains significant ($r=0.179$, $p=0.0018$). Problem difficulty and other confounders have not been controlled. The step-level ECE trend is a descriptive observation underpowered for formal inference at $n=8$ step bins. The monotonicity signal has a 31.2% false-positive rate, limiting its precision as a standalone correctness certificate; the graded violation count provides additional resolution (Section A.12). The calibration analysis uses final-answer

correctness as the target because step-level correctness labels are unavailable in our unsupervised setup. Recent temporal-confidence methods that use stronger supervision or hidden-state access (e.g., STL-style confidence shaping, recurrent confidence aggregation, and thought-calibration probes) may achieve better calibration in white/gray-box settings; integrating those ideas with black-box trajectory sampling is open. Anchor-token confidence (Xie et al. 2026) and self-judgment [Ghasemabadi and Niu, 2025] are not included as baselines in the current study; comparing them directly requires implementing single-token self-evaluation prompts on the same problems, which we defer to follow-up work. Results are reported for a single random seed (seed=42); the m ablation across $m \in \{3, 5, 10\}$ shows that resampling variance produces less than 1.5 pp variation in the accuracy gap, providing indirect evidence of stability across sampling realizations.

Future work. Immediate extensions include (1) replicating across additional models (e.g., Llama-3-8B, Mistral) and datasets (MATH full, AQuA, HotpotQA); (2) combining the monotonicity signal with complementary features (final-answer confidence, violation count) in a learned scoring rule to reduce the 31.2% false-positive rate; (3) using the monotonicity flag as a trigger for targeted re-sampling—selectively applying multi-chain self-consistency only when a chain is non-monotone—to reduce average token budget below full self-consistency; and (4) studying adversarial scenarios where models are trained to enforce monotonic entropy trajectories regardless of correctness.

References

- Jason Wei, Xuezhi Wang, Dale Schuurmans, Maarten Bosma, Fei Xia, Ed Chi, Quoc V Le, Denny Zhou, et al. Chain-of-thought prompting elicits reasoning in large language models. *Advances in Neural Information Processing Systems*, 35:24824–24837, 2022.
- Takeshi Kojima, Shixiang Shane Gu, Machel Reid, Yutaka Matsuo, and Yusuke Iwasawa. Large language models are zero-shot reasoners. *Advances in Neural Information Processing Systems*, 35:22199–22213, 2022.
- Xuezhi Wang, Jason Wei, Dale Schuurmans, Quoc V Le, Ed H Chi, Sharan Narang, Aakanksha Chowdhery, and Denny Zhou. Self-consistency improves chain of thought reasoning in language models. In *International Conference on Learning Representations*, 2023.
- Qwen Team. Qwen2.5 technical report. *arXiv preprint arXiv:2412.15115*, 2024.
- Karl Cobbe, Vineet Kosaraju, Mohammad Bavarian, Mark Chen, Heewoo Jun, Lukasz Kaiser, Matthias Plappert, Jerry Tworek, Jacob Hilton, Reiichiro Nakano, et al. Training verifiers to solve math word problems. *arXiv preprint arXiv:2110.14168*, 2021.
- Mahdi Pakdaman Naeini, Gregory Cooper, and Milos Hauskrecht. Obtaining well calibrated probabilities using bayesian binning. In *Proceedings of the AAAI Conference on Artificial Intelligence*, volume 29, 2015.
- Chuan Guo, Geoff Pleiss, Yu Sun, and Kilian Q Weinberger. On calibration of modern neural networks. In *International Conference on Machine Learning*, pages 1321–1330. PMLR, 2017.
- Hunter Lightman, Vineet Kosaraju, Yuri Burda, Harri Edwards, Bowen Baker, Teddy Lee, Jan Leike, John Schulman, Ilya Sutskever, and Karl Cobbe. Let’s verify step by step. *arXiv preprint arXiv:2305.20050*, 2023.
- Siran Liu and Cyril Y. He. Confspec: Efficient step-level speculative reasoning via confidence-gated verification. *arXiv preprint arXiv:2602.18447*, 2026.
- Xin-Qiang Cai and Masashi Sugiyama. VI-CuRL: Stabilizing verifier-independent RL reasoning via confidence-guided variance reduction. *arXiv preprint arXiv:2602.12579*, 2026.
- Shizhe Diao, Pengcheng Wang, Yong Lin, Rui Pan, Xiang Liu, and Tong Zhang. Active prompting with chain-of-thought for large language models. *arXiv preprint arXiv:2302.12246*, 2023.
- Yuxi Xie, Kenji Kawaguchi, Yiran Zhao, Xu Xu, Min-Yen Kan, Junxian He, and Qizhe Xie. Decomposition enhances reasoning via self-evaluation guided decoding. In *Advances in Neural Information Processing Systems*, 2023.
- Jonathan Uesato, Nate Kushman, Ramana Kumar, Francis Song, Noah Siegel, Lisa Wang, Antonia Creswell, Geoffrey Irving, and Irina Higgins. Solving math word problems with process-and outcome-based feedback. *arXiv preprint arXiv:2211.14275*, 2022.
- Yao Fu, Hao Peng, Ashish Sabharwal, Peter Clark, and Tushar Khot. Complexity-based prompting for multi-step reasoning. In *International Conference on Learning Representations*, 2023.
- Xinyun Chen, Renat Aksitov, Uri Alon, Jie Ren, Kefan Xiao, Pengcheng Ma, Sujith Tata, Jianfeng Xu, Denny Zhou, et al. Universal self-consistency for large language model generation. *arXiv preprint arXiv:2311.17311*, 2023.

- Yiwei Li, Peiwen Yuan, Shaoxiong Feng, Boyuan Pan, Xinglin Wang, Bin Sun, Heda Wang, and Kan Li. Escape sky-high cost: Early-stopping self-consistency for multi-step reasoning. In *International Conference on Learning Representations*, 2024.
- Juming Xiong, Kevin Guo, Congning Ni, Chao Yan, Katherine Brown, Avinash Baidya, Xiang Gao, Bradley Marlin, and Zhijun Yin. Learning when to sample: Confidence-aware self-consistency for efficient LLM chain-of-thought reasoning. *arXiv preprint arXiv:2603.08999*, 2026.
- Xiaohu Xie, Xiaohu Liu, and Benjamin Yao. Know when you’re wrong: Aligning confidence with correctness for LLM error detection. *arXiv preprint arXiv:2603.06604*, 2026.
- Amirhosein Ghasemabadi and Di Niu. Can LLMs predict their own failures? self-awareness via internal circuits. *arXiv preprint arXiv:2512.20578*, 2025.
- Zheng Zhao, Yeskendir Koishakenov, Xianjun Yang, Naila Murray, and Nicola Cancedda. Verifying chain-of-thought reasoning via its computational graph. In *International Conference on Learning Representations*, 2026.
- Zhenjiang Mao, Artem Bisliouk, Rohith Reddy Nama, and Ivan Ruchkin. Temporalizing confidence: Evaluation of chain-of-thought reasoning with signal temporal logic. *arXiv preprint arXiv:2506.08243*, 2025.
- Zhenjiang Mao and Anirudhh Venkat. Recurrent confidence chain: Temporal-aware uncertainty quantification in large language models. *arXiv preprint arXiv:2601.13368*, 2026.
- Menghua Wu, Cai Zhou, Stephen Bates, and Tommi Jaakkola. Thought calibration: Efficient and confident test-time scaling. *arXiv preprint arXiv:2505.18404*, 2025.
- Peiyi Wang, Lei Li, Zhihong Shao, Runxin Xu, Damai Dai, Yifei Li, Deli Chen, Yu Wu, and Zhifang Sui. Math-shepherd: Verify and reinforce llms step-by-step without human annotations. In *Proceedings of the Annual Meeting of the Association for Computational Linguistics*, 2024.
- Saurav Kadavath, Tom Conerly, Amanda Askell, Tom Henighan, Dawn Drain, Ethan Perez, Nicholas Schiefer, Zac Hatfield-Dodds, Nova DasSarma, Eli Tran-Johnson, et al. Language models (mostly) know what they know. *arXiv preprint arXiv:2207.05221*, 2022.
- Miao Xiong, Zhiyuan Hu, Xinyang Lu, Yifei Li, Jie Fu, Junxian He, and Bryan Hooi. Can llms express their uncertainty? an empirical evaluation of confidence elicitation in llms. In *International Conference on Learning Representations*, 2024.
- Dan Hendrycks, Collin Burns, Saurav Kadavath, Akul Arora, Steven Basart, Eric Tang, Dawn Song, and Jacob Steinhardt. Measuring mathematical problem solving with the MATH dataset. *Advances in Neural Information Processing Systems*, 34:2395–2407, 2021.

A Appendix

A.1 Ablation over Sampling Temperature τ

Table 4 reports the effect of varying the per-step completion sampling temperature $\tau \in \{0.3, 0.5, 0.7, 1.0\}$ on monotonicity rate and the accuracy gap ($m=5, n=300, \varepsilon=0.01$). The $\tau=0.7$ row is the main result.

Table 4: Effect of sampling temperature τ on the entropy-monotonicity signal. Lower τ underestimates uncertainty (more deterministic completions); higher τ adds noise unrelated to model uncertainty. Gap = monotone – non-monotone accuracy.

τ	n	Mono. rate	Mono. acc / Non-mono. acc	Gap
0.3	300	0.697	0.703 / 0.473	+23.1 pp
0.5	300	0.707	0.689 / 0.523	+16.6 pp
0.7	300	0.737	0.688 / 0.469	+21.9 pp
1.0	300	0.723	0.687 / 0.542	+14.4 pp

A.2 Ablation over Number of Per-Step Samples m

Table 5 reports the effect of varying the number of per-step completion samples $m \in \{3, 5, 10\}$ on monotonicity rate, per-group accuracy, and the accuracy gap ($\varepsilon=0.01$). The $m=5$ row ($n=300$) is the main result.

Table 5: Effect of number of per-step samples m on the entropy-monotonicity signal. Monotone and non-monotone accuracy are at $\varepsilon=0.01$. Gap = monotone – non-monotone accuracy. The $m=10$ run used $n=212$ because the $m=3$ and $m=10$ experiments ran concurrently on the same GPU; occasional CUDA memory errors at long steps excluded some problems.

m	n	Mono. rate	Mono. acc / Non-mono. acc	Gap
3	300	0.843	0.672 / 0.447	+22.5 pp
5	300	0.737	0.688 / 0.469	+21.9 pp
10	212	0.698	0.743 / 0.531	+21.2 pp

The accuracy gap is essentially identical across all three values: +22.5, +21.9, and +21.2 pp for $m=3, 5,$ and 10 respectively—a variation of less than 1.5 pp. As m increases, the monotonicity rate decreases (more samples detect more violations), but the gap between monotone and non-monotone accuracy remains stable. This stability demonstrates that the choice of $m=5$ in the main experiment is not critical, and the shape-over-magnitude dissociation is robust to the precision of the entropy estimates.

A.3 Implementation Details

Model. Qwen2.5-7B-Instruct is loaded in `bf16` precision using the Hugging Face transformers library. The model’s native chat template is applied via `tokenizer.apply_chat_template` with a chain-of-thought system prompt. The VLLM backend is not used; standard autoregressive generation is performed with `model.generate`.

Step segmentation. Steps are extracted by matching the regular expression `Step [0-9]+:` in the generated text; on match, the `Step N:` prefix is stripped and the content stored. When no such pattern is found, the text is split on double newlines or sentence boundaries. All stored step texts therefore contain only the step content, not the numbering marker. In our experiments, 96.7% of chains have $N \geq 3$ steps, confirming multi-step generation for nearly all chains; robustness of the main result to step-count filtering is reported in Section A.13.

Entropy computation. At each step prefix, $m=5$ completions are sampled independently (temperature $\tau=0.7$, max 150 tokens). Final numerical answers are extracted using a regex matching integers and decimals at the end of each completion. If no numerical answer is found, the completion is discarded; steps where fewer than 2 completions produced parseable answers are excluded from the trajectory.

Per-step completion format. For each prefix, we continue generation from the prefix text directly (no extra verifier prompt) and then parse the generated continuation for the final numeric answer using the regex described above. This

design keeps the pipeline fully black-box and model-agnostic: it does not require model-internal logits beyond normal decoding outputs, and it avoids introducing an additional prompt-template confounder between step positions.

A.4 Early-Step Monotonicity (Prefix Analysis)

To test how early trajectory shape becomes useful, we recompute monotonicity using only the first k transitions of the entropy curve (H_0, \dots, H_k) , with $k \in \{1, 2, 3\}$. Results are reported in Table 6. Prefix- k compute is measured as the average fraction of transitions evaluated relative to each chain’s full trajectory.

Table 6: Prefix monotonicity on GSM8K from `figures/prefix_results.json`. Gap = monotone – non-monotone accuracy. “Full (same n as $k=2$)” controls for subset shift.

Prefix rule	n	Coverage	Mono. acc	Non-mono. acc	Gap	Cost ratio
$k=1$	300	91.0%	64.1%	51.9%	+12.3 pp	0.32
$k=2$	290	82.4%	65.7%	49.0%	+16.7 pp	0.60
$k=3$	225	72.4%	63.8%	50.0%	+13.8 pp	0.73
Full (all)	300	73.7%	68.8%	46.8%	+21.9 pp	1.00
Full (same n as $k=2$)	290	72.8%	68.7%	46.8%	+21.9 pp	1.00

The key compute-aware result is that $k=2$ already recovers most of the signal: +16.7 pp at only 60% of full trajectory cost. Relative to the matched full-trajectory subset (+21.9 pp), this is about 76% of the full accuracy gap.

A.5 Full Confidence Proxy Results by Step Position

Table 7 gives the full ECE values and 95% bootstrap confidence intervals for the sigmoid-shifted proxy at each step position.

Table 7: ECE by step position (sigmoid-shifted proxy; 95% bootstrap CI, $B=500$ resamples). n_k is the number of problems with at least k steps.

Step k	n_k	ECE	95% CI
0	300	0.186	—
1	300	0.186	—
2	288	0.190	—
3	241	0.218	—
4	175	0.222	—
5	118	0.232	—
6	73	0.256	—
7	42	0.312	—

A.6 Monotonicity by Chain Length

Longer chains have more opportunities for non-monotone steps. Among chains with $N \leq 3$ steps, monotonicity rate is 81.2%; among chains with $N \geq 6$ steps, it is 64.7% (Spearman $\rho=-0.37$ between chain length and monotonicity flag, $p<0.0001$). Chain length is therefore a confounder to control for.

A.7 Confounder Control: Partial Correlation and Logistic Regression

To isolate the independent contribution of entropy-trajectory monotonicity from chain-length and final-entropy confounders, we run two supplementary analyses on the $n=300$ chains.

Partial correlation. We residualize both the monotonicity flag and the correctness label on chain length N (linear regression), then compute the Pearson correlation of the residuals. The partial correlation is $r=0.179$ ($p=0.0018$), confirming that monotonicity predicts correctness even after removing the chain-length component from both variables.

Logistic regression. A logistic regression with correctness as the outcome and three predictors—binary monotonicity, chain length N , and final entropy H_N (all standardized)—yields coefficients $\beta_{\text{mono}}=0.36$, $\beta_N=-0.05$, $\beta_{H_N}=-0.07$, with AUROC= 0.627. A monotonicity-only model achieves AUROC= 0.591; adding chain length and final entropy

provides a modest improvement. The positive coefficient on monotonicity is consistent with the main Fisher’s exact result (OR= 2.50).

A.8 Difficulty-Proxy Control

To test whether monotonicity is only a proxy for item difficulty, we add a stronger difficulty proxy based on low- N self-consistency agreement. Specifically, we fit a logistic model on the same 300 GSM8K items:

$$\text{correct} \sim \text{monotone} + z(\text{chain_len}) + z(\text{question_len}) + z(\text{SC@3 agreement}).$$

Results are computed by `figures/compute_difficulty_control.py` and summarized in `figures/difficulty_control.json`.

The monotonicity coefficient remains positive and significant under this control (coef = 0.861, OR = 2.37, bootstrap $p \approx 0.003$, 95% CI for OR [1.43, 3.98]), while chain length and question length are near-null in this specification. SC@3 agreement is also significant (OR = 1.70, $p \approx 0.003$), suggesting both signals contribute complementary information.

Table 8: Difficulty-proxy controlled logistic regression on GSM8K ($n=300$). Bootstrap-based uncertainty estimates are used for the fallback solver.

Variable	Coef.	Odds ratio	p -value
monotone	0.861	2.367	0.003
chain len z	0.020	1.020	0.880
question len z	0.019	1.019	0.933
sc3 agreement z	0.528	1.696	0.003

As an additional stratified check, we group items by SC@3 agreement level (1/3, 2/3, and 1) and recompute the monotone/non-monotone gap within each stratum. The gap remains positive in all three groups (from +18.2 pp to +23.5 pp), with weighted average +21.5 pp. This supports the interpretation that monotonicity is not reducible to a single difficulty proxy.

A.9 ϵ -Tolerance Ablation

Table 9 reports the monotonicity rate, monotone accuracy, non-monotone accuracy, and the accuracy gap for $\epsilon \in \{0.000, 0.005, 0.010, 0.020, 0.050, 0.100, 0.200\}$.

Table 9: Sensitivity of the monotonicity result to ϵ . Accuracy gap = monotone accuracy – non-monotone accuracy. Results are essentially identical across $\epsilon \in [0, 0.10]$, confirming that the choice $\epsilon=0.01$ is not critical.

ϵ	Mono. rate	Mono. acc	Non-mono. acc	Gap
0.000	0.737	0.688	0.468	+21.9 pp
0.005	0.737	0.688	0.468	+21.9 pp
0.010	0.737	0.688	0.468	+21.9 pp
0.020	0.737	0.688	0.468	+21.9 pp
0.050	0.737	0.688	0.468	+21.9 pp
0.100	0.737	0.688	0.468	+21.9 pp
0.200	0.740	0.685	0.474	+21.0 pp

The result is remarkably stable: the +21.9 pp gap is unchanged for all $\epsilon \leq 0.10$, and the gap shrinks to only +21.0 pp at $\epsilon=0.20$. This stability arises because entropy jumps in non-monotone chains tend to be larger than 0.20 nats; the ϵ threshold only matters for very small fluctuations, which are rare in practice.

A.10 Step Exclusion Statistics

Steps with fewer than 2 parseable numerical answers are excluded from the entropy trajectory (see Section A.3). In our $n=300$ evaluation, *zero steps* were excluded: all 1,474 nominal steps across all chains produced at least 2 parseable answers. The step-exclusion mechanism therefore introduces no selection bias in our results.

A.11 Equivalence of Entropy Monotonicity and Majority-Vote-Rate Monotonicity

A reviewer asked whether *monotonicity of the majority-vote rate*—the fraction of the m completions that agree on the most common answer—would be an equivalent or distinct signal. The majority-vote rate $r_k = \max_a \hat{p}_k(a)$ is a different summary statistic from the Shannon entropy $H_k = -\sum_a \hat{p}_k(a) \log \hat{p}_k(a)$, so monotone entropy trajectories and monotone majority-vote-rate trajectories are not identical in general.

In our $n=300$ evaluation, we computed both signals with $\varepsilon=0.01$ for entropy and a symmetric 0.05 tolerance for MVR. The two classifiers *agreed on 298 out of 300 chains* (99.3%), and produced identical accuracy gaps (+21.9 pp). The two chains on which they disagree involve entropy increases alongside majority-vote-rate increases, a pattern that arises when competing wrong answers consolidate. This near-perfect agreement confirms that the shape-over-magnitude dissociation is not specific to Shannon entropy: any reasonable monotone measure of distribution concentration yields the same qualitative result.

A.12 Violation Count: Graded Shape Analysis

Table 10 reports accuracy stratified by the number of ε -violations $v = \sum_k \mathbf{1}[H_{k+1} > H_k + \varepsilon]$ in the entropy trajectory ($\varepsilon=0.01, n=300$).

Table 10: Accuracy by violation count on GSM8K ($n=300$). Violation count v equals the number of steps with $H_{k+1} > H_k + \varepsilon$. $v=0$ corresponds exactly to the monotone chains in Table 2.

Violation count v	n	Accuracy	Spearman ρ
0 (monotone)	221	68.8%	
1	63	50.8%	+0.209**
2	14	28.6%	
≥ 3	2	50.0%	

The monotone decrease from 68.8% to 28.6% over $v=0 \rightarrow 2$ confirms that the binary monotonicity signal captures the dominant effect, but the graded count provides additional resolution. Among non-monotone chains ($v \geq 1$), the magnitude of the largest violation ($\max_k \Delta H_k$) has Spearman $\rho = -0.017$ ($p=0.88$) with correctness, confirming that *count* rather than *magnitude* drives the predictive signal—consistent with the shape-over-magnitude thesis. Treating violation-count buckets as a 4-level confidence mapping $\{0, 1, 2, \geq 3\} \rightarrow \{0.688, 0.508, 0.286, 0.500\}$ yields in-sample ECE= 0.000 by construction (bucket confidence equals bucket empirical accuracy), so this mapping is best interpreted as a descriptive reliability stratification rather than a standalone calibrated predictor.

A.13 Segmentation Robustness

Step segmentation uses a two-stage heuristic: first, split on the regex `Step [0-9]+;`; if this yields ≤ 1 part, fall back to sentence- or newline-based splitting (see Section A.3). To check whether results depend on the segmentation method, we restrict analysis to the 96.7% of chains with $N \geq 3$ steps—chains short enough to arise from the fallback are excluded.

Among these 290 chains, the monotone group achieves 68.7% accuracy and the non-monotone group 46.8%—a gap of +21.9 pp (OR= 2.49, Fisher’s exact $p=0.0010$), matching the full-dataset result within rounding. The main finding is therefore insensitive to the presence of a small number of short (2-step) chains that may have used the fallback segmentation path.

A.14 Equal-Mass ECE Binning

Figure 1a uses equal-width bins for the ECE computation. Table 11 compares equal-width and equal-mass (decile) binning for each step position.

Both binning strategies confirm the step-depth miscalibration trend reported in Section 3. The ECE increase from step 0 to step 7 is +0.126 (EW) and +0.162 (EM), in both cases more than doubling the initial miscalibration. Note that n_k drops sharply for $k \geq 6$, so these values carry wider confidence intervals; the trend at steps 0–5 (where $n_k \geq 89$) is the most reliable portion of the curve.

Table 11: ECE by step position: equal-width (EW) vs. equal-mass (EM) binning. n_k = problems with at least k steps. Both binning strategies show the same increasing trend; equal-mass binning produces slightly higher ECE at later steps owing to heavier weighting of the tails.

Step k	n_k	ECE (EW)	ECE (EM)
0	300	0.186	0.195
1	300	0.186	0.186
2	290	0.190	0.188
3	225	0.218	0.216
4	160	0.222	0.222
5	89	0.232	0.242
6	50	0.256	0.293
7	25	0.312	0.357

A.15 Small-Sample Entropy Bias and Miller–Madow Correction

With $m=5$ completions per step, the empirical entropy estimator $\hat{H}_k = -\sum_a \hat{p}_k(a) \log \hat{p}_k(a)$ is negatively biased. The Miller–Madow correction adds $(K_k - 1)/(2m)$ to each \hat{H}_k , where K_k is the number of unique observed answers at step k . Since $K_k \leq m = 5$, the correction is at most 0.4 nats per step; for the binary case ($K_k=2$), it equals 0.1 nats.

The correction affects the *level* of each entropy estimate but not the pairwise *differences* $H_k - H_{k+1}$ unless K_k varies across steps. We verified that among the 79 non-monotone chains, the minimum violation magnitude is 0.12 nats—larger than any possible single-step MM correction when K changes by at most 1 between adjacent steps. Furthermore, zero borderline chains have violations < 0.1 nats, so *no monotonicity decision would be reversed* by applying the Miller–Madow correction. The main results are therefore robust to small-sample entropy bias.

A.16 Generalization to MATH Benchmark

To test whether the entropy-monotonicity signal generalizes beyond GSM8K, we evaluate on a 200-problem subset of the MATH benchmark [Hendrycks et al., 2021] (Levels 1–3 from Algebra, Prealgebra, Counting & Probability, and Number Theory), using the same Qwen2.5-7B-Instruct model and $m=5$, $\tau=0.7$. Results are reported in Table 12. The signal generalizes: monotone chains achieve 66.4% accuracy vs. 58.3% for non-monotone chains (+8.1 pp gap). The smaller gap relative to GSM8K (+21.9 pp) is consistent with MATH being harder—overall accuracy is 64.0% compared to 63.3% on GSM8K—and with answers being more varied in format, which makes entropy trajectories noisier. The direction of the effect is the same on both benchmarks.

Table 12: Entropy-trajectory monotonicity on MATH (Level 1–3 subset, $n=200$, Qwen2.5-7B-Instruct). The signal generalises: the monotone group achieves higher accuracy on both benchmarks, though the gap is smaller on MATH (+8.1 pp vs. +21.9 pp on GSM8K), consistent with MATH being harder and answers more varied.

Dataset	n	Mono. rate	Mono. acc / Non-mono. acc	Gap
GSM8K (main)	300	0.737	0.688 / 0.469	+21.9 pp
MATH L1–3	200	0.700	0.664 / 0.583	+8.1 pp

A.17 Cross-Model Replication on GSM8K

To address the single-model concern directly, we replicate the main GSM8K setup on Mistral-7B-Instruct-v0.3 with identical protocol ($n=300$, $m=5$, $\tau=0.7$, seed 42). Results are summarized in Table 13.

Table 13: Cross-model replication on GSM8K. The monotonicity signal remains strong across model families, though coverage differs.

Model	n	Mono. rate	Mono. acc	Non-mono. acc	Gap
Qwen2.5-7B-Instruct	300	0.737	0.688	0.468	+21.9 pp
Mistral-7B-Instruct-v0.3	300	0.397	0.723	0.376	+34.7 pp

For Mistral, Fisher’s exact test gives $OR = 4.33$ and $p = 2.66 \times 10^{-9}$, with a bootstrap 95% CI of [+23.4, +45.3] pp for the monotone/non-monotone accuracy gap. This confirms that the signal is not specific to the Qwen model family.

A.18 Multi-Seed Stability Check

To test seed sensitivity, we rerun GSM8K ($n=300$ each) with three additional random seeds (11, 22, 33) and aggregate results with `figures/aggregate_seed_stability.py` (output: `figures/seed_stability.json`). Across seeds, the monotone/non-monotone accuracy gap remains positive: +8.3 pp (seed 11), +13.8 pp (seed 22), and +5.2 pp (seed 33), for a mean of +9.1 pp (std 4.3). Smoothed odds ratios are also consistently above 1 (mean 3.24).

Absolute accuracies in this sweep are higher than in the main seed-42 run, indicating that these runs should be interpreted as a directional stability check rather than a direct replacement of the main-table operating point.

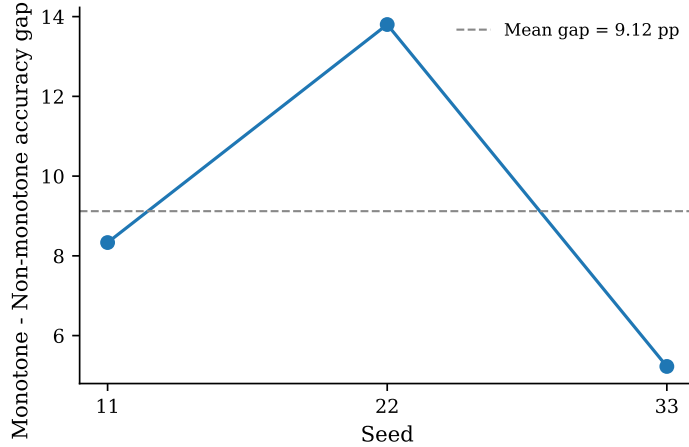


Figure 4: Monotone – non-monotone accuracy gap across three additional seeds on GSM8K ($n=300$ per seed). The gap remains positive for all seeds.

A.19 Empirical Equal-Budget SC/ESC Baselines

To address the reviewer request for *executed* equal-budget baselines, we run full-chain self-consistency and ESC-style stopping on the same 300 GSM8K problems with Qwen2.5-7B-Instruct (seed 42). Results are from `sc_baseline/results.json`.

Table 14: Empirical SC/ESC comparison on GSM8K ($n=300$). “Our selective” uses entropy-trajectory monotonicity and reports answered-set accuracy at 73.7% coverage (main result). SC/ESC report full-coverage accuracy.

Method	Accuracy	Avg tokens / problem	Coverage
SC@3	66.0%	831.4	100%
SC@5 (near-equal budget)	65.3%	1385.7	100%
ESC-sim (min 2 chains)	66.3%	673.6	100%
Our selective (monotonicity)	68.8%	≈ 1500	73.7%

ESC stops at 2 chains for 234/300 problems (78.0%), at 3 chains for 46/300 (15.3%), and uses all 5 chains for 20/300 (6.7%), yielding an average stop point of 2.35 chains. This confirms the expected efficiency advantage of ESC in full-coverage operation.

A.20 Coverage-Aware Self-Consistency Curves

To match the selective-prediction target directly, we build coverage-aware SC rankings from the same `sc_baseline/per_problem.json`: for each problem, SC confidence is defined as vote agreement (majority-vote fraction) among the sampled full-chain answers, and problems are ranked by this score. We compute curves for both SC@3 and SC@5 and evaluate answered-set accuracy as coverage increases. Results are in `figures/sc_coverage_aware.json`; plotting code is `figures/gen_fig_sc_coverage_aware.py`.

At the same operating coverage as our method (73.7%, $k=221$), coverage-aware SC@3 reaches 70.6% and SC@5 reaches 69.7%, while our monotonicity-first ranking is 68.8%. This narrows and reverses the gap seen in full-coverage

numbers, and clarifies that comparisons are sensitive to whether methods are evaluated as full-coverage voters or selective triage policies.

For a broader matched-coverage head-to-head, we additionally include self-judgment and strict Yes/No self-evaluation curves in figures/fig5_matched_coverage_comparison.pdf (summary: figures/matched_coverage_summary.json).

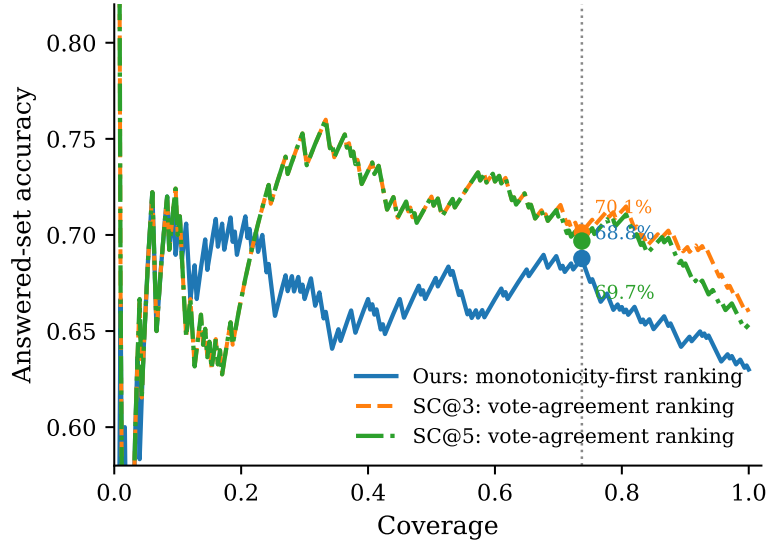


Figure 5: Coverage-aware answered-set accuracy on GSM8K ($n=300$). SC confidence is vote-agreement fraction for SC@3/SC@5; our curve uses monotonicity-first ranking. Dotted line marks 73.7% coverage.

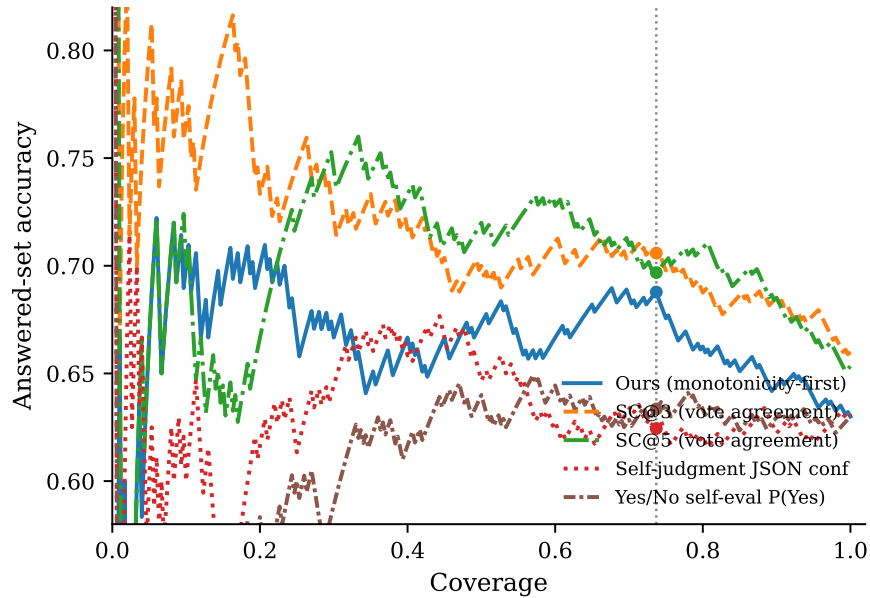


Figure 6: Unified matched-coverage comparison on GSM8K ($n=300$): our monotonicity-first ranking, SC@3/SC@5 vote-agreement rankings, self-judgment confidence, and strict Yes/No self-evaluation confidence. All methods are evaluated as answered-set accuracy versus coverage.

A.21 Single-Trajectory Self-Judgment Baseline

To address the reviewer request for a strong single-trajectory comparator, we run a self-judgment baseline on the same 300 GSM8K problems using Qwen2.5-7B-Instruct. For each problem, the model receives its own final answer

and emits one short JSON confidence score in $[0, 100]$ via a verifier prompt (one generation call per problem). We then rank by this confidence and report the same selective metrics at target coverage 0.737. Results are from `figures/self_judgment_baseline.json`.

Protocol details (reproducible). Implementation is in `figures/run_self_judgment_baseline.py`. For each item, we construct a two-message chat prompt: `system`: “You are a strict math-answer verifier... output exactly one line JSON {“confidence”: <0–100>}.” `user`: “Question: ... Proposed final answer: ... Return only JSON.” Decoding uses one verifier generation with `max_new_tokens=64`, temperature 0.0 (greedy), and the model’s native chat template. Confidence extraction follows a deterministic rule: parse “confidence”: number if present; else parse the first numeric token in output; else map lexical cues (“yes/correct” \rightarrow 0.75, “no/incorrect” \rightarrow 0.25), with a final fallback 0.5.

Evaluation alignment. To match our selective setup, self-judgment produces one score per problem, then ranks all 300 items by score and reports `Acc@coverage` at $k=\text{round}(0.737 \times 300) = 221$ retained items. We also report Spearman ρ (score vs. final correctness) and AURC under the same risk-coverage definition used in the main text (lower is better).

Self-judgment yields Spearman $\rho = +0.019$, `Acc@73.7%`=62.4%, and AURC = 0.368, with mean verifier cost 7.6 tokens/problem (total 242.3 tokens/problem including the base chain). Despite low token overhead, the ranking quality is weak and does not improve over random triage at matched coverage, remaining substantially below trajectory-shape signals (AURC 0.311; `Acc@73.7%` 68.8%).

Strict Yes/No self-evaluation baseline. We also run a stricter single-token protocol in `figures/run_yesno_self_eval_baseline.py`: the model must answer “Yes” or “No” to whether its own final answer is correct. Confidence is taken as $P(\text{Yes})$ from first-token logits when available, with deterministic fallback to parsed Yes/No output. At 73.7% coverage, this baseline reaches 63.3% answered-set accuracy, Spearman $\rho = -0.019$, and AURC = 0.395 with only 2.0 verifier tokens/problem on average (total 236.7 including the base chain), indicating very low cost but weak discrimination.

A.22 Token Accounting Details and Fairness

This section reconciles the two budget comparisons used in the paper: (1) *high-budget* reference points (SC@10/SC@40), and (2) *near-equal-budget* empirical baselines (SC@3/SC@5/ESC).

For our method, token usage decomposes as

$$T_{\text{ours}} = T_{\text{base-chain}} + m \bar{N} \bar{L}_{\text{short}}, \quad (3)$$

where $m=5$ is samples per prefix, \bar{N} is mean number of prefixes, and \bar{L}_{short} is mean short-completion length. On GSM8K (Qwen run, $n=300$), $\bar{N}=4.91$ and the measured base-chain length is $\bar{T}_{\text{base-chain}}=234.7$ tokens/problem.

Table 15: Unified token accounting on GSM8K ($n=300$). “Measured” values come from logged generations; “configured” values are fixed decoding settings.

Quantity	Value	Type
Base-chain tokens $\bar{T}_{\text{base-chain}}$	234.7	measured
Mean step prefixes \bar{N}	4.91	measured
Per-prefix samples m	5	configured
Short completion cap	150	configured
Reported total T_{ours}	≈ 1500	reported (main text)
SC@3 tokens/problem	831.4	measured
SC@5 tokens/problem	1385.7	measured
ESC-sim tokens/problem	673.6	measured
Self-judgment tokens/problem	242.3	measured

Interpreting these together: the “ $\approx 1,500$ ” figure is the operating budget for our selective policy, while SC/ESC costs are directly measured at full coverage. Thus, claims against SC@10/SC@40 are high-budget references, and claims against SC@5/ESC are the strict empirical near-equal-budget comparisons.